

# Correlated Supernova Systematics and Ground Based Surveys

Alex G. Kim<sup>1</sup> and Eric V. Linder<sup>1,2,3</sup>

<sup>1</sup>*Lawrence Berkeley National Laboratory, Berkeley, CA 94720 USA*

<sup>2</sup>*University of California, Berkeley, CA 94720, USA*

<sup>3</sup>*Institute for the Early Universe, Ewha Womans University, Seoul, Korea*

(Dated: May 2, 2017)

Supernova distances provide a direct probe of cosmic acceleration, constraining dark energy. This leverage increases with survey redshift depth at a rate bounded by the systematic uncertainties. We investigate the impact of a wavelength-dependent, global correlation model of systematics in comparison to the standard local-redshift correlation model. This can arise from subclass uncertainties as features in the supernova spectrum redshift out of the observer photometric filters or spectral range. We explore the impact of such a systematic on ground-based supernova surveys such as Dark Energy Survey and LSST, finding distinctive implications. Extending the wavelength sensitivity to  $1.05\ \mu\text{m}$  through “extreme red” CCDs can improve the dark energy figure of merit by up to a factor 2.

## I. INTRODUCTION

Type Ia supernovae (SNe) are standardizable distance indicators that can be seen to high redshift, over at least 70% of the lookback time of the universe. In a given galaxy, they occur on  $10^2$ – $10^3$  year time scales, so for  $10^{10}$  galaxies in the visible universe this implies one SN per second. A three-year deep survey could theoretically detect  $10^8$  SNe so if the distance to each were known to 20% (0.46 mag; i.e. no standardization applied, just identification as Type Ia), then one could attain 0.01% distance measurements in 25 equal-error distance bins statistically. In this sense SNe are the most powerful cosmological probe statistically.

However, as for any probe, the key issue comes down to systematic uncertainties not statistics. For SNe, such uncertainties include flux calibration, dust corrections, and population drift. Numerous articles have addressed one or another of these, for various experimental designs [1]. Some uncertainties can be removed by using spectrophotometry rather than filter measurements; others can be ameliorated by observations spanning a long wavelength range; others by “like to like” comparison of time-series or spectral features [2, 3].

To allow general comparison of different SN surveys, a phenomenological systematic model offers a compact way of summarizing the specifics of the measurement and analysis chain that delivers distances. It also provides a basis with which to identify previously unknown sources of uncertainty. Specifically, the model can contain parameters describing the distribution of supernova subsets, e.g. magnitude offsets, that when fit can be checked for deviations or inconsistencies.

A key feature of such a model would be a systematic floor, reflecting that the large number of SNe mentioned above should not in reality give an asymptotically small precision. This is fundamentally different from “self calibration” – adopting a fixed parametric form and simultaneously fitting the error parameters along with the cosmology [17]. Self calibration only holds if there is no uncertainty in the form, only the parameters. This is a

weaker meaning of systematic uncertainty, and in general we do not have strong confidence in the form for population drift, for example. Therefore we consider a systematics model that explicitly includes a floor.

A well-used systematics model was introduced by [6], consisting of local correlations between SNe within redshift bins of width 0.1. Large numbers of SNe in a bin reduce the distance error to a finite floor, but continued cosmological leverage could be obtained by adding independent SNe, those in another redshift bin [18]. The floor is given in magnitudes by

$$\sigma \equiv 5 \log \frac{\delta d}{d} = \sigma_{\text{sys}} \frac{1+z}{1+z_{\text{max}}}, \quad (1)$$

where  $d$  is the luminosity distance,  $z$  is the redshift of the bin center, and  $z_{\text{max}}$  is the maximum redshift of the survey; we refer to this as the LH systematics model. An important feature is that the floor does not vanish even for  $z = 0$ . The cosmological parameter estimation results are fairly insensitive to the bin width (scaling the error amplitude as the inverse square root of the width) within the range  $\Delta z = 0.05 - 0.4$  [7].

However, we want to explore beyond this local correlation model, where only SNe within a restricted redshift range are correlated with each other. One can imagine that some systematics might correlate all SNe, or all SNe above a certain redshift (e.g. if they rely on near-infrared observations). This can give a more global correlation, and we consider a model for that here.

In Sec. II we present a motivated model for correlated systematic uncertainties, and in Sec. III propagate its effects through to dark energy cosmology fitting, especially the dark energy equation of state figure of merit. We investigate in particular the influence of various survey and supernovae characteristics on the figure of merit. Section IV extends this to error fitting and to error models describing population drift. The results are summarized in Sec. V.

## II. CORRELATED SYSTEMATIC

An error model with every supernova potentially correlated with every other supernova is general, but one should use some physical motivation to guide the form of the correlations[19]. Our systematic model is based on SN spectral characteristics and says that errors, once they enter the measurements, affect all SNe above the entry redshift. We consider several different error contributions, each with their own entry redshift. This correlates that portion of the systematic uncertainty completely among all higher redshift SNe. The error matrix can be viewed as being “laid down” in steps, with the first error source contributing  $\sigma_1^2$  to all elements of the error matrix, the second error source adding  $\sigma_2^2$  to the matrix block corresponding to higher redshift SNe, and so on for even higher redshift SNe. Effectively, the error matrix has a “wedding cake” form, climbing in steps from the upper left to lower right.

Such an error structure naturally arises as supernova light redshifts out of the range of observational sensitivity. For example, the SN Ia subclassification scheme of Branch et al. (2006) [8] identifies four groups based on the equivalent widths of absorption features at rest-frame 5750 and 6100 Å (from Si II), and the presence of high-velocity Ca II IR3 absorption at 8000 Å. All three lines are available for  $z < 0.12$  candidates from ground-based spectroscopic observations within the  $0.35 \mu\text{m} < \lambda < 0.9 \mu\text{m}$  atmospheric window.

The spectral features contribute to the standardization of the SNe as distance indicators; this can be viewed as calibrating the SN absolute magnitude  $M$ . As one by one the spectral features become inaccessible beyond  $z = 0.12, 0.47,$  and  $0.57$ , supernovae at higher redshifts incur additional error floors from imperfect marginalization over each lost calibration parameter. This produces an error model where progressively higher redshift bins share additive correlated uncertainties. Note that even with measurements of these spectral features, the ensemble of supernova distances is still expected to have a correlated error floor due to systematic limitations of such a classification scheme in general.

The principles of a wavelength dependent, globally correlated systematic can be extended to the larger set of spectral features cited in the literature as indicators of SN Ia diversity [9]. Moreover, since relevant features generally have large equivalent widths (due to the high velocities in the exploding supernova), they may show up in broadband photometry as well. The bounded observer window also induces redshift-dependent correlations in broadband photometric analysis from propagated uncertainties of SN and dust models at common restframe wavelengths. We therefore investigate application of such a correlated systematics model to surveys involving either broadband photometry or spectroscopic followup.

Mathematically, the SN absolute magnitude is taken to be determined as a function of measurements of  $N$  spectral indicators. At higher redshifts, some of these,

say  $N - i$  redder indicators, are unavailable. This leads to increased magnitude uncertainty, and a covariance in magnitude (and hence distance) errors of

$$\langle \delta M_a \delta M_b \rangle = \sigma_{\text{int}, n_a}^2 \delta_{ab} + V_{ab}, \quad (2)$$

where the intrinsic dispersion enters as a diagonal contribution  $\sigma_{\text{int}}^2$  (generally dependent on the procedure used to determine  $M$  for each supernova), and

$$V_{ab} = \sum_{i=\max(n_a, n_b)}^N \sigma_{N-i+1}^2. \quad (3)$$

The indices  $a, b$  label individual SNe and  $n_a$  is the number of spectral features observed for supernova  $a$ . The more spectral information, the fewer terms contribute to the sum and the smaller the overall uncertainty. However note that we always keep a base variance  $\sigma_1^2$ .

An example covariance matrix for three error sources (and five SNe in increasing redshift order) is shown below:

$$V = \begin{pmatrix} \sigma_1^2 & \sigma_1^2 & \sigma_1^2 & \sigma_1^2 & \sigma_1^2 \\ \sigma_1^2 & \sigma_1^2 & \sigma_1^2 & \sigma_1^2 & \sigma_1^2 \\ \sigma_1^2 & \sigma_1^2 & \sigma_1^2 + \sigma_2^2 & \sigma_1^2 + \sigma_2^2 & \sigma_1^2 + \sigma_2^2 \\ \sigma_1^2 & \sigma_1^2 & \sigma_1^2 + \sigma_2^2 & \sigma_1^2 + \sigma_2^2 & \sigma_1^2 + \sigma_2^2 \\ \sigma_1^2 & \sigma_1^2 & \sigma_1^2 + \sigma_2^2 & \sigma_1^2 + \sigma_2^2 & \sigma_1^2 + \sigma_2^2 + \sigma_3^2 \end{pmatrix}. \quad (4)$$

Another way to achieve the same result is to view the table of error contributions for each SN as a  $N_{\text{SN}} \times N_{\text{err}}$  matrix. The product of this with its transpose will automatically give a positive definite, symmetric matrix. That is, let

$$S = \begin{pmatrix} \sigma_1 & 0 & 0 \\ \sigma_1 & 0 & 0 \\ \sigma_1 & \sigma_2 & 0 \\ \sigma_1 & \sigma_2 & 0 \\ \sigma_1 & \sigma_2 & \sigma_3 \end{pmatrix}. \quad (5)$$

Then the product  $V = SS^T$  gives Eq. (4). Here we see that each row gives the systematic error summary of a SN, and each column represents a different systematic error contribution. So all SNe suffer from uncertainty type 1, with magnitude  $\sigma_1$  (representing that even with the identified spectral features there will be residual, unidentified systematics); only the last three SNe (which could represent higher redshifts) suffer from type 2 uncertainty, and only the last SN (e.g. highest redshift) has type 3 uncertainty. Thus, the fourth SN gets contributions from type 1 and 2 uncertainties, while the fifth SN has systematics of types 1, 2, and 3. This is easily generalized to  $N_{\text{err}}$  contributions to the systematic uncertainty and to  $N_{\text{SN}}$  supernovae. Such an error list, arising from a linear combination of independent uncertainties (similar to a Karhunen-Loeve transform), produces the wedding cake type of covariance matrix seen in Eq. (4), and we call this the KL systematics model.

The amplitudes of the uncertainties can be expressed either in terms of the individual  $\sigma_j$  or in terms of the

covariance matrix entries

$$\Sigma_i^2 = \sum_1^i \sigma_j^2. \quad (6)$$

For definiteness, and to compare the results to the commonly used, diagonal LH systematic model, we explore the case where

$$\Sigma_i^2 = \sigma_{\text{LH}}^2(\langle z_i \rangle). \quad (7)$$

For the ground-based survey we assume  $\sigma_{\text{LH}}(z) = 0.03(1+z)/1.9$  and here  $\langle z_i \rangle$  is the average redshift of the SNe within the range where  $\sigma_i$  (but not yet  $\sigma_{i+1}$ ) enters. In the limit that  $N_{\text{err}}$  equals the number of independent error bins used in the LH model, the diagonal elements of the KL and LH covariance matrices are the same.

### III. EFFECT ON COSMOLOGY FIT

We now explore the implications of the KL correlated systematic model on the cosmological parameter estimation.

#### A. Cosmology and Survey Parameters

We consider a survey with 2000 SNe uniformly distributed between  $z = 0.1 - z_{\text{max}}$ , supplemented with an additional 300 SNe at  $z = 0.03 - 0.1$ . The values of  $z_{\text{max}}$  considered are 0.6, 0.7, 0.8, 0.9. The distance modulus covariance matrix consists of a diagonal contribution from an intrinsic dispersion  $\sigma_{\text{int}} = 0.1$  for each supernova and a correlated part given by the KL systematic model. We explore several KL scenarios with different  $N_{\text{err}}$  and entry redshifts for each error, but in all cases the amplitude of the systematics is fixed by Eq. (7). The statistical measurement uncertainty is taken to be subdominant. To speed up our analysis, we combine supernovae in 0.1 redshift bins and use the average distance modulus with variance  $\sigma_{\text{int}}^2/n_i$ , where  $n_i$  is the number of SNe in each bin. (Such a procedure is found to make negligible difference to the final result.) We include a CMB Planck prior on the distance to last scattering.

The cosmological fit parameters of interest are the matter density  $\Omega_m$  in units of the critical density, and the dark energy equation of state parameters  $w_0$  and  $w_a$  where  $w(a) = w_0 + w_a(1-a)$ . Spatial curvature is taken to vanish. The fiducial model is a flat  $\Lambda$ CDM cosmology with  $\Omega_m = 0.28$ . The combination  $\mathcal{M}$  of the SN absolute magnitude and Hubble constant is also fit. We examine the impact of different systematic error cases on the dark energy figure of merit  $\text{FOM} = 1/\sqrt{\det C_{w_0 w_a}}$ , where  $C_{w_0 w_a}$  is the  $2 \times 2$  submatrix of the parameter covariance matrix (inverse Fisher matrix).

In Sec. IV A we carry out a  $\chi^2$  fit rather than a Fisher matrix analysis, finding the results agree well. We also consider there the case where the  $\sigma_i$  are fit simultaneously with the cosmology.

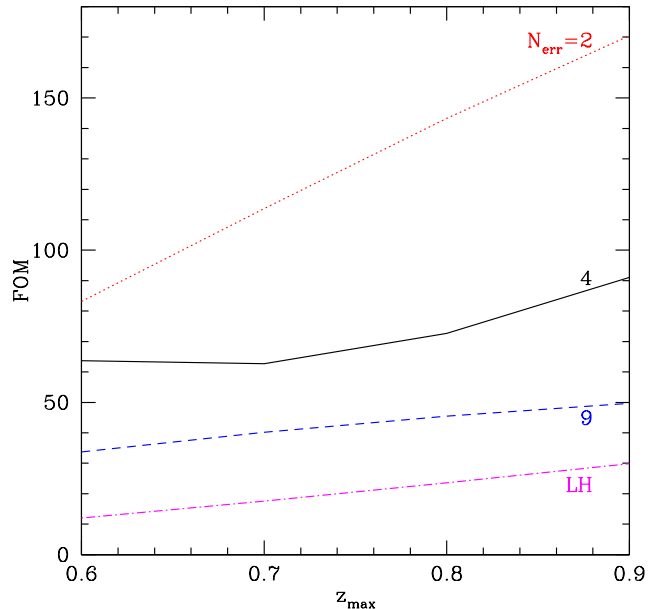


FIG. 1: The dark energy figure of merit (FOM) is plotted vs survey redshift depth  $z_{\text{max}}$  for different cases of the global systematic model. Adding more error layers, each appearing above its corresponding redshift, lowers the FOM for surveys extending beyond those redshifts. The LH local systematics model has a worse FOM because SNe in different redshift bins do not see correlated contributions among its 9 errors.

#### B. Impact of Survey Characteristics

A first point of interest is the behavior of the cosmological parameter estimation as we include various uncertainties, i.e. as  $N_{\text{err}}$  changes. When  $N_{\text{err}} = 1$ , then all elements of the error matrix are identical, corresponding to completely correlated uncertainty across all SNe and all redshifts; this only affects the uncertainty on the absolute magnitude parameter  $\mathcal{M}$ , not any of the cosmological parameters. When the off-diagonal elements are not all equal, as for  $N_{\text{err}} > 1$ , then the values of each  $\sigma_i$  are relevant.

The number of features contributing systematic uncertainties is important. Figure 1 shows the effect of both the number of error levels and the maximum depth of the survey on the FOM.

For the  $N_{\text{err}} = 2$  case, we take the second error to come in at  $z = 0.1$ ; this can either reflect the highest wavelength (Ca II) spectral feature or be viewed as the difference between a separate, local ( $z < 0.1$ ) SN survey that may be carried out spectrophotometrically (e.g. Nearby Supernova Factory [10]) and a high redshift ground based SN survey such as Dark Energy Survey (DES [11]) or LSST [12]. Note that the  $N_{\text{err}} = 9$  and LH systematics cases both have new errors appearing every 0.1 in redshift, and in fact have identical diagonal

terms in the correlation matrix. However, the global correlation causes more of the effect of the uncertainties to propagate into the absolute magnitude parameter, ameliorating their influence on the cosmological parameter determination, and so giving a higher FOM.

We take for our canonical systematic model the case mentioned in Sec. II where the redshifting of important Si II and Ca II spectral features out of the observed wavelength range generates systematic uncertainties. For sensitivity diminishing at  $0.9\mu\text{m}$  these occur at  $z = 0.12, 0.47, 0.57$ . This is referred to as the  $N_{\text{err}} = 4$  case since the error matrix will be built up out of 4 layers, i.e. blocks involving  $\Sigma_1^2$  through  $\Sigma_4^2$ . The following quantitative results use this model.

Most interestingly, the KL systematic, if it holds as a better description of SN observations for ground based observations than the uncorrelated LH systematic, predicts (for  $N_{\text{err}} = 4$ ) a factor of 3 greater FOM for comprehensive surveys extending to  $z_{\text{max}} = 0.9$ . Moreover, the constraints in the dark energy equation of state  $w_0$ - $w_a$  plane have slightly more complementarity with other probes such as weak lensing or baryon acoustic oscillations than in the LH case.

Considering the number  $N$  of well-characterized SNe in the survey, we find that the FOM does not saturate with number as severely as in the LH systematic case. Instead, we have

$$\text{FOM} \sim N^{1/2}, \quad (8)$$

over the range considered; for very large  $N$  it gradually levels off. In the purely statistical error case  $\text{FOM} \sim N$  but recall that in addition to these  $N$  SNe at  $z = 0.1$ – $z_{\text{max}}$  we include a constant 300 SNe at  $z = 0.03$ – $0.1$  and a Planck CMB prior on the distance to last scattering. We emphasize that the  $N$  SNe represent those with spectral or sufficiently high signal to noise photometric information to discern the different spectral feature classes down to the level of the  $\Sigma_{\text{sys}}(z) = 0.03(1+z)/1.9$  systematic. Figure 2 shows the FOM as a function of  $N$ .

Regarding the amplitude of the systematics, in the canonical case, the errors are  $\{\sigma_i\} = (0.0167, 0.0117, 0.0130, 0.0133)$ . The more correlated we make the SN uncertainties, by raising  $\sigma_1$ , the less the effect of the remaining errors on the cosmological parameters. Figure 3 illustrates this, where we adjust  $\sigma_1$  to be either 0.02 (which drives  $\sigma_2$  nearly to 0, i.e.  $\Sigma_2 \rightarrow \Sigma_1$  due to the constraint of Eq. 7) or 0 (making  $\sigma_2 = 0.020$ ). The area of the  $w_0$ - $w_a$  contour clearly decreases as more of the systematic becomes global, and interestingly the degeneracy direction rotates slightly to become more complementary to other probes such as weak lensing and baryon acoustic oscillations.

Studying the highest redshift systematic uncertainty  $\sigma_4$ , we find an analogous effect on the FOM, as seen in Fig. 4. As  $\sigma_4 \rightarrow 0$ ,  $\Sigma_4 \rightarrow \Sigma_3$  and the SNe above  $z = 0.47$  all have a coherent systematic. This improves the FOM by 33%. Thus, tight control of systematics out to the highest redshifts is beneficial. As  $\sigma_4$  is instead increased,

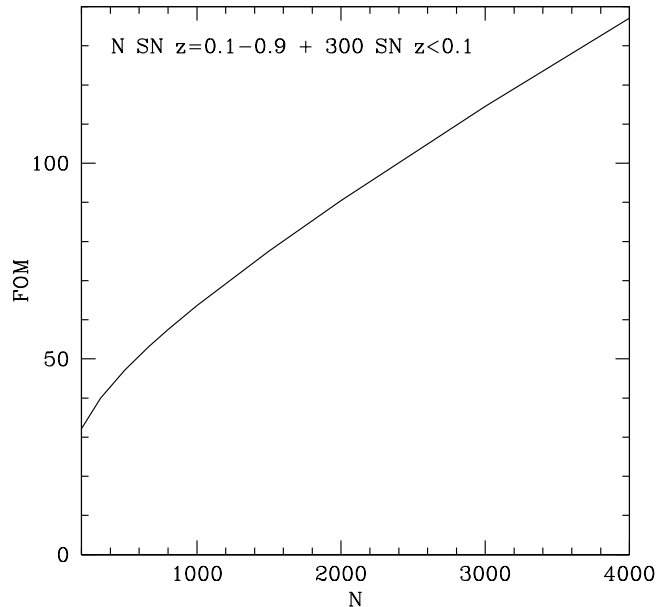


FIG. 2: The dark energy figure of merit (FOM) is plotted vs number  $N$  of well-characterized SNe in the high-redshift survey. The canonical FOM for  $N = 2000$  changes by factors 1.5 or 0.7 for  $N$  doubling or halving, respectively.

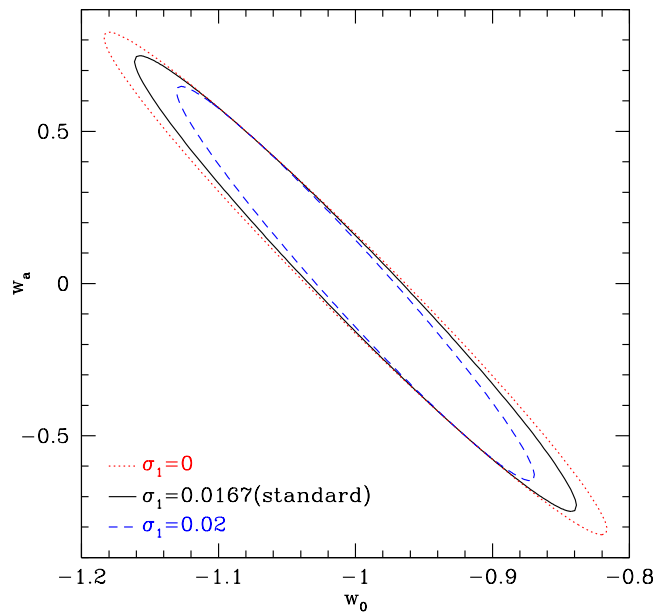


FIG. 3: 68% confidence level contour in the dark energy equation of state plane is shown for varying levels of the global systematic  $\sigma_1$ . The sum  $\Sigma_2^2 = \sigma_1^2 + \sigma_2^2$  stays fixed. As  $\sigma_1$  approaches  $\Sigma_2 = 0.0204$ ,  $\sigma_2 \rightarrow 0$  and the SNe out to  $z = 0.47$  share a common systematic, propagating mostly into  $\mathcal{M}$  rather than dark energy parameters. Thus the contour tightens. Conversely, as  $\sigma_1 \rightarrow 0$ , the SNe become less correlated and the constraints weaken.

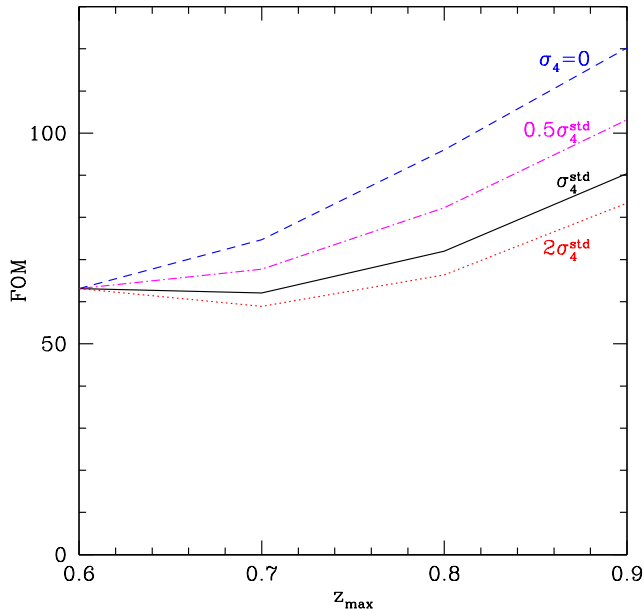


FIG. 4: The dark energy figure of merit (FOM) is plotted for different values of the highest redshift systematic  $\sigma_4$ . If the spectral feature at  $5750 \text{ \AA}$  responsible for  $\sigma_4$  is not actually relevant to SN magnitudes, so  $\sigma_4 \rightarrow 0$ , then the correlation in magnitude uncertainty among the highest redshift SNe grows and the FOM improves. Larger systematics lower the FOM at all redshifts beyond  $z = 0.6$  where this error enters. Here  $\sigma_4^{\text{std}}$  is the canonical value  $0.0133$  given by Eq. (7).

the FOM worsens, but slowly, with a doubling of  $\sigma_4$  (30% increase in  $\Sigma_4$ ) causing an 8% decline in FOM. Since  $\sigma_4$  enters at  $z = 0.57$ , the FOMs for all values of  $\sigma_4$  agree up to this redshift; generally the FOM then flattens with survey depth as the impact of the new error enters. At even higher redshift the FOM gradually increases as the leverage from a larger redshift baseline asserts itself. Note however that the FOM can actually decrease with  $z_{\text{max}}$  if the error is large enough to overwhelm the redshift leverage.

Since the SN properties whose lack of measurement is responsible for the systematic uncertainties enter at observed wavelengths that increase for higher redshift SNe, an extension of the wavelength region over which the survey is sensitive would forestall the loss of information due to missed features. This is of course one of the main reasons for considering space-based SNe surveys. But within the context of ground-based surveys, if we could slightly extend the wavelength region over which high signal to noise measurements could be made, this could pay dividends for cosmological parameter reach.

The ongoing development of “extreme red” CCDs [13], detectors with enhanced efficiency out to  $1\mu\text{m}$  or even  $1.05\mu\text{m}$ , offers the possibility of recovering from some of the observing inefficiencies caused by bright atmospheric emission and absorption at longer wavelengths. We con-

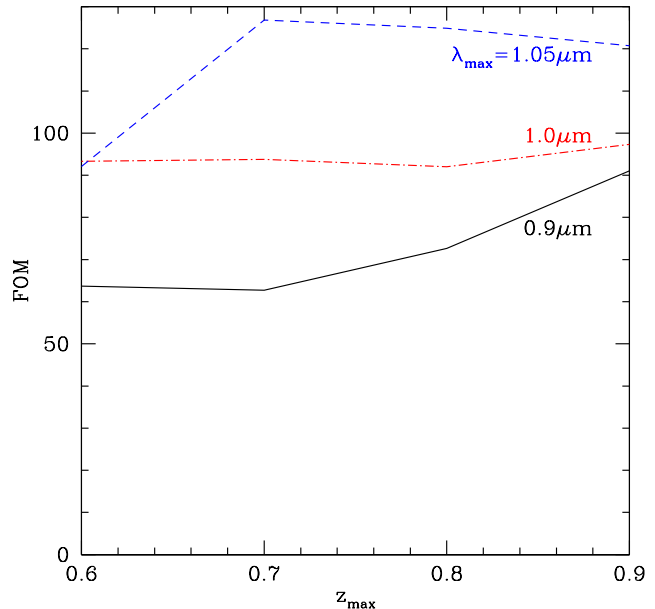


FIG. 5: The dark energy figure of merit (FOM) is plotted vs survey redshift depth  $z_{\text{max}}$  for different values of the wavelength sensitivity cutoff. Increasing the wavelength range can give substantial improvements to FOM, even for shallower surveys.

sider these two cases in addition to the standard  $0.9\mu\text{m}$  cutoff. Figure 5 shows that such technology advances could have dramatic effects on dark energy science.

The general effect of a systematic error contribution is to suppress the growth of FOM with redshift at the redshift corresponding to where the spectral feature leaves the observational sensitivity window. That is, the curves in the figure flatten at the redshifts where the errors enter, as mentioned above. For the  $\lambda_{\text{max}} = 0.9\mu\text{m}$  case, all the errors have entered by  $z = 0.57$  and so the FOM curve, although starting low due to the accumulated systematics, increases with  $z_{\text{max}}$ . For the  $\lambda_{\text{max}} = 1\mu\text{m}$  case, the errors appear at  $z = 0.25, 0.64,$  and  $0.74$ , hence the FOM curve is roughly flat over the range of  $z_{\text{max}}$  shown. For  $\lambda_{\text{max}} = 1.05\mu\text{m}$ , the errors come in at  $z = 0.31, 0.72, 0.83$  so the FOM is able to climb with redshift out to  $z_{\text{max}} = 0.7$  and then levels off.

Compared to the canonical  $z_{\text{max}} = 0.9$  case the improvement in FOM by extending sensitive measurements to  $\lambda_{\text{max}} = 1$  or  $1.05\mu\text{m}$  is 7% or 32% respectively. Moreover a survey with extreme red sensitivity to  $1.05\mu\text{m}$  is equally powerful at  $z_{\text{max}} = 0.7$  vs  $0.9$  (recall the number of SNe is kept constant at  $N = 2000$ ), giving there a factor of 2 improvement in FOM over a standard  $0.9\mu\text{m}$  cutoff survey.

## IV. FURTHER APPLICATIONS

### A. Error Fitting

Systematics represent the residuals after known errors are taken into account. One usually estimates, either empirically through training and validation subsets or using simulation and modeling guidance, the level of the systematic. An example is the 0.03 mag amplitude in the LH model. In Sec. III we assume that those levels are already well-characterized when incorporated in the distance modulus covariance matrix. Alternatively, within the cosmology fit one can simultaneously estimate the level of variance or introduce new parameters to fit out the effect of the systematic.

To explore this we carry out simultaneous fits to various systematics model parameters along with the cosmological parameters. In place of the Fisher analysis, we use MINUIT [14] for parameter fitting and the resultant Hessian matrix to calculate the FOM. Contributions to the fit likelihood come from not only the usual  $\chi^2$  term but also a penalty term  $\ln \det C$  involving the covariance matrix  $C$ . For example, this approach was carried out to fit the intrinsic SN dispersion  $\sigma_{\text{int}}$  by [15]. We do not bin but analyze the full uniformly-distributed 2000 SNe plus the 300 local SNe. Since we are interested in fit uncertainties, when possible we do not realize dispersion on the simulated data to ensure that the best fit and input parameters are identical. We restrict these studies to the  $N_{\text{err}} = 4$ ,  $z_{\text{max}} = 0.9$  case.

We first check that this likelihood approach gives the same results as the Fisher analysis for our canonical case. The FOMs agree to better than 5%.

Next, we consider that the estimate of the absolute magnitude may have a different intrinsic dispersion depending on the number of spectral features used in its estimate. This is done by considering the  $\sigma_{\text{int},n_a}^2$  in Eq. (2) as (four) fit parameters rather than assuming they equal 0.1. Since we are fitting for variances, we must instantiate dispersion in the simulated data. We perform only one instantiation as a single fit is time consuming with a  $2300 \times 2300$  matrix inversion in each likelihood evaluation. The uncertainty found for each  $\sigma_{\text{int},n_a}$  is  $\sim \text{few} \times 10^{-2}$ , the level to which we can detect real differences in the absolute magnitude models. The FOM is within 3% of the fixed  $\sigma_{\text{int}} = 0.1$  case.

The correlated systematics  $\sigma_i$  reflect the residual uncertainties in the absolute magnitude offsets in redshift bins defined by spectral-feature visibility. These  $N_{\text{err}}$  offsets can be fit for simultaneously with the cosmology since the luminosity distance model is smooth, without sudden steps (see the next subsection for the case of a smooth magnitude drift). Fitting for the biases on  $M_i$  (without the  $V$  term in the covariance matrix), the realizations of  $\delta M_i$  are determined to  $\sim 10^{-2}$  and the FOM falls to 59 (i.e. by  $\sim 40\%$ ). However, when adopting the  $\sigma_i$  given by Eq. (7) as priors on  $\delta M_i$  (with mean 0), the realizations of  $M_i$  are determined to  $\sim 7.5 \times 10^{-3}$  and

the FOM improves to 102 (by 12%). The smooth Hubble diagram of the cosmological parameters allows the self-calibration of magnitude offsets, leading to an improved FOM over the canonical case.

### B. Population Drift

As used so far, the KL model assumes that once information on a spectral feature is lost, the uncertainty enters and remains constant with redshift. In terms of a magnitude correction based on that feature, this makes sense: no information means no correction and hence the added uncertainty. But we can also consider the spectral feature as aiding classification of subtypes of SNe Ia with different absolute magnitudes.

The various subtypes will all combine to give some average absolute magnitude for the sample. With the loss of information, the proportion of subtypes is unlikely to suddenly change abruptly, and so the average should initially remain a good approximation. At higher redshifts, however, the population fractions may drift further and so the previous average becomes increasingly uncertain as an estimate of the true sample average. In this population drift interpretation, the systematic uncertainty increases as the redshift increases beyond that where the feature is lost.

We explore a modified KL model where the systematic scales as

$$\sigma_i(z) = \sigma_{i\star} \frac{z - z_i}{z_\star - z_i} \quad (9)$$

in the error table  $S$ . The exception is  $\sigma_1$  which we take to be a global uncertainty for SN standardization. The covariance matrix then contains elements

$$\begin{aligned} \langle \delta M_a \delta M_b \rangle = & \sigma_1^2 \\ & + \sum_{i=2}^{N - \min(n_a, n_b) + 1} \sigma_{i\star}^2 \left( \frac{z_a - z_i}{z_\star - z_i} \right) \left( \frac{z_b - z_i}{z_\star - z_i} \right), \end{aligned} \quad (10)$$

where  $z_a$ ,  $z_b$  are the redshifts of the two SNe being correlated and  $z_i$  is the entry redshift of the systematic  $\sigma_i$ .

The systematic  $\sigma_i$  is thus not a constant entry in a wedding cake layer but rather gives a ramp up: it starts at 0 when it enters at  $z_i$  and attains an amplitude  $\sigma_{i\star}$  at  $z = z_\star = 0.9$ . For comparison we choose  $\sigma_{i\star}$  to equal the  $\sigma_i$  as given for the redshift independent, or flat, KL model in the earlier part of the paper to match the LH model amplitudes. Due to the scaling with  $z$ , the systematic amplitude will be less than the flat KL case for all  $z < z_\star$ . Not surprisingly, therefore the FOM for the scaling case is larger (by 28% in the canonical  $N_{\text{err}} = 4$ ,  $z_{\text{max}} = 0.9$  case). This implies that such population drift systematics have less effect (for the same amplitude at the maximum redshift) than the magnitude correction systematic.

## V. CONCLUSIONS

Systematics are the ultimate limiting factor in any cosmological probe. We show that uncertainties due to the loss of information of supernova spectral features can correlate distance errors for all redshift higher than where the information is lost. One expects such loss in ground-based surveys where sensitivity declines strongly beyond 9000 Å.

Such correlation in the error model can actually have a tempering effect, relative to a localized uncertainty such as in the LH model, in that a wider range of supernovae experience the effect, it propagates mostly into the absolute magnitude determination, and so the impact on the cosmological parameter estimate is reduced. For the same level of dispersion (autocovariance), the KL correlated systematic model allows a larger dark energy figure of merit and slower approach to the systematic floor.

Extending the wavelength sensitivity into the near infrared, such as may be possible with new technology “extreme red” CCDs that also cover the optical region, has science potential that should be considered in mission designs. For a survey depth of  $z_{\max} = 0.9$  the gain in figure of merit is 32% on going out to  $1.05 \mu\text{m}$ . Moreover, the same FOM can be achieved even if the survey depth is  $z_{\max} = 0.7$ , since the added systematics beyond  $z = 0.72$  due to loss of Si II features counteract the increased redshift baseline, for a fixed number of supernovae.

Viewing spectral information loss as opening the analysis to uncorrected population drift, we find that this does not have as much impact as for the magnitude correction

ansatz. As redshift increases, information might also be gained from rest frame UV features, but this would occur at low redshift ( $z \approx 0.1-0.25$ ) and is not expected to have much impact on survey depth design. Currently the situation concerning UV features for magnitude correction, or their ability to substitute for the higher wavelength information discussed here, is not clear.

The calculations here are meant illustratively, to show the method and possible impacts of correlated systematics. We do not claim that the Branch et al. model [8] for supernova subclassification is truth, that those particular wavelengths carry the essential information on supernova magnitudes. For example, Bailey et al. [16] have identified certain distinct series of spectral flux ratios and ranked their correlation with absolute magnitude. Nevertheless, the approach of analyzing correlated systematics, and the benefit of extending the wavelength range, e.g. through red sensitive CCDs, should be general.

## Acknowledgments

We acknowledge useful discussions with David Rubin. AK thanks the Institute for the Early Universe for hospitality. This work has been supported in part by the Director, Office of Science, Office of High Energy Physics, of the U.S. Department of Energy under Contract No. DE-AC02-05CH11231, and the World Class University grant R32-2009-000-10130-0 through the National Research Foundation, Ministry of Education, Science and Technology of Korea.

- 
- [1] P. Astier, J. Guy, R. Pain, & C. Balland, *Astron. Astrophys.*, 525, A7 (2011).  
L. Faccioli et al., *Astropart. Phys.* accepted [arXiv:1004.3511]  
A. G. Kim, E. V. Linder, R. Miquel, & N. Mostek, *Mon. Not. R. Astron. Soc.*, 347, 909 (2004).  
M. C. March, R. Trotta, L. Amendola, & D. Huterer, arXiv:1101.1521 (2011).  
J. Nordin, A. Goobar, J. Jönsson, *J. Cosmol. Astropart. Phys.*, 2, 8 (2008).  
N. Mostek, Ph.D. Thesis (2007).  
<http://sites.google.com/a/lbl.gov/njmostek/docs/PhD.pdf>  
J. Samsing, & E. V. Linder, *Phys. Rev. D*, 81, 043533 (2010).
- [2] D. Branch, S. Perlmutter, E. Baron, P. Nugent, arXiv:astro-ph/0109070
- [3] E. V. Linder, *Phys. Rev. D* 79, 023509 (2009). [arXiv:0812.0370]
- [4] A. G. Kim & R. Miquel, *Astropart. Phys.* 24, 451 (2006). [arXiv:astro-ph/0508252]
- [5] L. Faccioli et al., *Astropart. Phys.* accepted [arXiv:1004.3511]
- [6] E. V. Linder & D. Huterer, *Phys. Rev. D* 67, 081303 (2003). [arXiv:astro-ph/0208138]
- [7] E. V. Linder, *Phys. Rev. D* 75, 063502 (2007). [arXiv:astro-ph/0612102]
- [8] D. Branch et al. *PASP* 118, 560 (2006). [arXiv:astro-ph/0601048]
- [9] V. Arsenijevic, S. Fabbro, A. M. Mourão & A. J. Rica da Silva, *Astron. Astrophys.*, 492, 535 (2008).  
S. Bailey et al., *Astron. Astrophys.*, 500, L17 (2009).  
S. Blondin, K. S. Mandel, & R. P. Kirshner, *Astron. Astrophys.*, 526, A81 (2011).  
S. Benetti, et al., *Astrophys. J.*, 623, 1011 (2005).  
R. S. Ellis et al., *Astrophys. J.*, 674, 51 (2008)  
R. J. Foley et al., *Astrophys. J.*, 684, 68 (2008).  
J. Nordin, et al, *Astron. Astrophys.*, 526, A119 (2011).  
X. Wang, et al. *Astrophys. J. Lett.*, 699, L139 (2009).
- [10] Nearby Supernova Factory <http://snfactory.lbl.gov>
- [11] Dark Energy Survey <http://www.darkenergysurvey.org/>
- [12] Large Synoptic Survey Telescope <http://www.lsst.org/lsst>
- [13] C. Bebek, private communication
- [14] Minit <http://www.cern.ch/minuit>
- [15] A. Kim, *PASP*, in press [arXiv:1101.3513]
- [16] S. Bailey et al., *Astron. Astrophys.* 500, L17 (2009). [arXiv:0905.0340]
- [17] We note that this is effectively what happens with SN light curve fitting parameters. Some approaches fit for the SN parameters first, deriving distances, and then use

those distances to fit for cosmology, but it can be more powerful to carry out the cosmology fit in one step [4, 5].

- [18] One can view the correlation of SNe within the redshift bin as a block diagonal component consisting of each of the individual SNe within the bin. That is, one does not have to bin the SNe per se, just correlate them. Having a  $1700 \times 1700$  error matrix of individual SNe, with each group of 100 between  $z = 0.1(i - 1)$  and  $0.1i$  where  $i =$

- $1, 2, \dots, 17$  say, correlated, hence giving a block diagonal structure, gives mathematically equivalent results to a  $17 \times 17$  diagonal matrix with the statistical error reduced by the square root of the number of SNe within the group.
- [19] Moreover, for an arbitrary set of correlations the covariance matrix is not guaranteed to give a positive definite result.